

15. IR Laser Chemistry and C–F Chromophore Absorption of 1,2-Dichloro-1,1,2-trifluoroethane

by Donald W. Lupo, Martin Quack*, and Beat Vogelsanger

Laboratorium für Physikalische Chemie, ETH-Zentrum, CH-8092 Zürich

Dedicated to *Hans H. Günthard* on the occasion of his 70th birthday

(25. IX. 86)

The photochemical-reaction yields after IR multiphoton excitation of $\text{CHFCl}-\text{CF}_2\text{Cl}$ are reported and evaluated in terms of the steady-state rate coefficient for reactant decay

$$k(\text{st}) = 10^{6.1 \pm 0.3} (I/\text{MWcm}^{-2}) \text{ s}^{-1}$$

The dominant primary reaction channels are α, β HCl and HF elimination, although minor pathways seem to include Cl_2 elimination and other channels, which are discussed. The major uncertainty in the comparison with theoretical estimates resides in the fraction of C–F chromophore band strength which contributes to excitation. The total band strength for the range from 940 cm^{-1} to 1310 cm^{-1} is reported to be $G = \int \sigma(\tilde{\nu}) (d\tilde{\nu}/\tilde{\nu}) = 8.2 \text{ pm}^2$.

1. Introduction. – Most of the results reported in the young field of IR laser chemistry still concern qualitative effects and observations, but quantitative data are becoming increasingly important [1–4], in particular in relation to potential technical applications. A recent review has shown that there is a severe lack of quantitative IR photochemical rate parameters, which are urgently needed [4].

The primary kinetic quantity in IR laser chemistry is the rate coefficient, which may depend upon fluence

$$F = \int_0^t I dt \quad (1)$$

intensity I , and time, in general:

$$k_{\text{um}}(F, I, t) = -\frac{d \ln F_{\text{R}}}{dt} \quad (2)$$

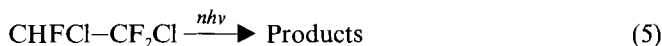
$F_{\text{R}} = c(t)/c(0)$ is the remaining fraction of reactant molecules. It has been shown [5] [6] that the steady-state limit of the rate coefficient can be obtained from bulk measurements of the primary photochemical reaction yield as a function of well defined fluence under controlled irradiation conditions but without ns time resolution, in case B [5] with an approximately intensity-proportional value:

$$\lim_{\substack{I = \text{const.} \\ t \rightarrow \infty}} k(t) = k(\text{st}) = k_f(\text{st}) \cdot I \quad (3)$$

$$k_f(\text{st}) = \lim_{\substack{t \rightarrow \infty \\ F \rightarrow \infty}} \left\{ - \left(\frac{d \ln F_{\text{R}}^*}{dF} \right) \right\} \quad (4)$$

The star indicates that the concentration measurements are carried out long after the laser pulse of total fluence F . The practical determination of $k(st)$ has been documented [4] [6]. The method has been checked recently by direct time-resolved measurements [7] [8].

Here, we report the measurement of the rate coefficient for the reaction



under irradiation with the R34 line of the pulsed CO_2 laser at $\tilde{\nu} = 1087 \text{ cm}^{-1}$. The primary channels are mainly HCl and HF eliminations, although evidence for other reaction channels has been found. To our knowledge, there has been no previous investigation of the IR laser chemistry of this compound, which seems to be poorly characterised spectroscopically as well; there exists only one uncommented report of the IR spectrum [9a]. The VUV (vacuum ultraviolet) photolysis of CHFCl–CF₂Cl has been studied [10]. The compound is of some potential interest for further investigations because of its potential as an anaesthetic [9b, c], its optical activity, inviting a study of the polarization dependence of IR laser chemistry, and because of the several competing reaction channels. The thresholds for the lowest channels have not been determined for this compound, but it can be inferred from studies on many related compounds that the threshold energy for HCl elimination is *ca.* 200 to 240 kJ mol⁻¹ and somewhat higher for HF elimination [11].

2. Experimental. – 1,2-dichloro-1,1,2-trifluoroethane was purchased from *PCR Research Chemicals*. The identity was confirmed by the IR spectrum [9], and GC showed a purity of 99.9%. We have also measured the vapour pressure as a function of temp. obtaining

$$\ln(P/\text{mbar}) = -18.05 - \frac{3362 \text{ K}}{T}$$

in the temp. range of 250–300 K. This gives a normal b.p. of 302 K, in agreement with the reported value of 301.3 K at 1013 mbar [9]. The substance was degassed by several freeze-pump-thaw cycles before use. N_2 and NO were purchased from *Sauerstoff- und Wasserstoffwerke Luzern* and from *Matheson*, respectively. There were visible amounts of NO_2 in the NO sample, but neither NO nor the impurities therein changed the product yield or chemistry, thus the NO was not further purified.

IR band strengths were measured on a *BOMEM DA.002* FTIR spectrometer at a substance pressure of 3.8–4 mbar and a resolution of 0.1 cm^{-1} using a 17-cm steel cell with KCl windows. Spectra were measured for the pure substance and in the presence of 800 mbar N_2 for pressure broadening.

The experimental arrangement for IR photochemical measurements has been described in detail in [6]. Samples were photolysed in the far field ($\approx 20 \text{ m}$) of a *Lumonics-TEA-103-2* line-tunable CO_2 laser equipped with unstable resonator optics, which yielded a nearly *Gaussian* spatial fluence profile after spatial filtering of side maxima. Samples were contained in a 10-cm steel cell with KCl or NaCl windows. N_2 was used as a buffer gas and NO as a check for radical reaction contributions to the product yield. Yields were analysed with a *Hewlett-Packard 5880A* gas chromatograph and a *Perkin-Elmer 983G* IR spectrometer. The dependence of product yield on partial pressure of CHFCl–CF₂Cl was investigated to check for thermal reactions [6]. The pressure conditions for the determinations of the frequency and fluence dependence of the yield (0.2 mbar CHFCl–CF₂Cl, 9.8 mbar buffer gas) were chosen such that thermal reactions were not important and that the absorption in the band at 999 cm^{-1} was strong enough to allow yield determination *via* quantitative IR spectroscopy. At partial pressures above 1 mbar, we observed a marked thermal contribution.

Measurements of the temporal pulse shape of the laser output were carried out with a photon drag detector (*Rofin*) and a transient digitiser (*Tektronix 7912AD*).

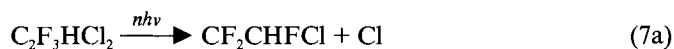
3. Results and Discussion. – 3.1. *Dissociation Channels in the IR Photolysis of CHFCl–CF₂Cl and Definition of the IR Photochemical Yield.* The most abundant products of the IR laser photolysis of CHFCl–CF₂Cl were found by IR spectroscopy and GC to be, in order of abundance, chlorotrifluoroethane ($\text{C}_2\text{F}_3\text{Cl}$), trifluoroethylene ($\text{C}_2\text{F}_3\text{H}$),

and 1,2-dichlorodifluoroethylene ($C_2F_2Cl_2$), in the ratio 6:4:1. The following possible primary reaction channels were considered:

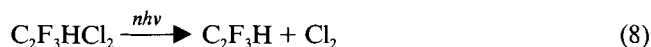
α,β HCl elimination:



C–Cl bond fission:



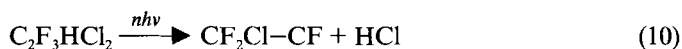
α,β Cl_2 elimination:



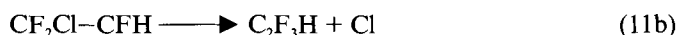
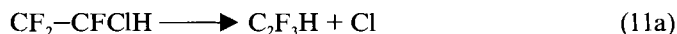
α,β HF elimination:



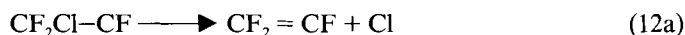
α,α HCl elimination:



Reactions 6, 8, and 9 are clean molecular eliminations leading to stable products, whereas *Reactions 7 and 10* produce reactive radicals. The products of *Reaction 7* may undergo further dissociation:



The product of *Reaction 10* may also react further:



or rearrange:



The products of *Reactions 6* and *9* may establish equilibrium with their fragments:



A significant contribution from *Equilibrium 13* would cause the observed HCl/HF branching ratio to be different from the primary ratio. In this case, however, C_2F_4 , which was not observed, should be present in the product mixture.

The observed reactant loss could be distorted beyond the primary photodissociation by radical-initiated thermal reactions:



If *Reactions 14* and *15* contributed significantly, the addition of a radical scavenger such as NO should lower the apparent yield. Under identical irradiation conditions and at the same total pressures, the yield was found to be the same with N₂ and with NO as buffer gases; this indicates that observed yields reflect only primary photochemical processes. In addition, the constancy of the C₂F₃Cl/C₂F₂Cl₂ ratio for NO and N₂ as buffer indicates that product ratio reflects the primary HCl/HF branching ratio. We do not consider α,α HCl elimination to be a significant channel because of the preponderance of the three major products, although small amounts of unidentified substances were detected.

The results do not distinguish clearly between molecular Cl₂ elimination and successive C–Cl bond breaking. The fact that NO did not alter the product distribution significantly indicates only that *either* molecular Cl₂ elimination dominates *or* that *Reaction 11* is faster than the scavenging of the products of C–Cl fission by NO. α,β Cl₂ eliminations are not commonly observed IR-photochemical phenomena, although α,α eliminations are known [12–14]. Though the results do not allow us to determine the primary channel leading to the loss of two Cl-atoms, they do show that the observed yields are indeed primary photochemical yields, which allow us to obtain *k*(st) summed over all reaction channels. The molecular channels certainly contribute dominantly overall.

The apparent total IR photochemical product yield P_{app} within the irradiated volume V₁ is defined as

$$P_{\text{app}} = f(V_c/V_1) \quad (16)$$

where V_c is the total cell volume and *f* is the fraction of reactant dissociated per pulse, obtained from

$$[\text{CHFCl}-\text{CF}_2\text{Cl}]_n = [\text{CHFCl}-\text{CF}_2\text{Cl}]_0(1-f)^n \quad (17)$$

for *n* laser pulses. V₁ is *defined* as the product of the path length and an effective beam cross section of constant fluence containing the total pulse energy. For a *Gaussian* profile V₁ is given by

$$V_1 = b \frac{\pi W^2}{2} \quad (18)$$

where *b* is the path length and *W* is the characteristic *Gaussian* width of the experimental fluence profile. (For further discussion, see [6].)

3.2. *Frequency Dependence of the Product Yield.* Fig. 1 contains both the absorption of CHFCl–CF₂Cl in the CO₂ laser emission region and the irradiation-frequency dependence of P_{app} at a nominal fluence of 4 J cm⁻². (Nominal fluence F₀ = F_{max} from the experimental near-*Gaussian* fluence profile [6].) We emphasise that the shape of the frequency dependence of the yield is to be viewed as a qualitative survey. In particular, the frequency dependence of P_{app} is *not* an indicator of frequency dependence in *k*(st); in an investigation of the IR photochemistry of (Z)–C₄F₈ one finds similar values for *k*(st) at four different laser lines, in spite of significant differences in P_{app} at the same nominal fluence [15].

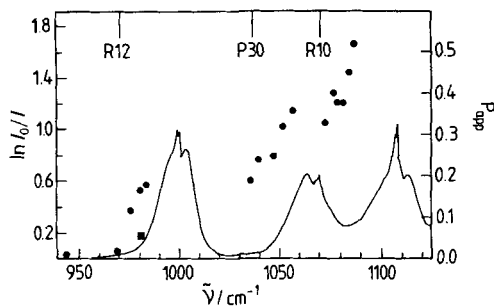


Fig. 1. The frequency dependence of P_{app} at a nominal fluence of 4 Jcm^{-2} . The circle at 981 cm^{-1} designates a discharge voltage of 27 kV, the square 37 kV.

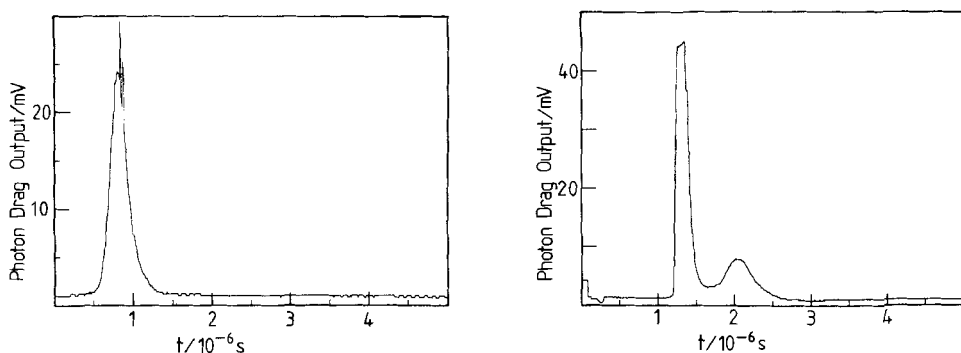


Fig. 2. Temporal pulse shapes for emission at 981 cm^{-1} (10R28), a) discharge voltage 27 kV; b) discharge voltage 37 kV

We call attention to the difference in P_{app} at 981 cm^{-1} (10R28) for low (27 kV, circle) and high (37 kV, square) laser-capacitor discharge voltages. This difference may be understood from Fig. 2, which displays typical temporal pulse shapes for low and high discharge voltages. Measurement of seven pulses at 37 kV showed an average of $22 \pm 6\%$ (90% confidence limit) of the total pulse energy to be contained in the low intensity N_2 tail, whereas there was no observable tail at 27 kV. As little or no dissociation is expected to result from radiation in the tail at 10 mbar, because of collisional quenching, this reduces the effective fluence at high discharge voltage, which reduces the product yield. This demonstrates that the usually reported apparent yields as a function of fluence (defined in a variety of ways, when defined at all) can be taken only as *qualitative* results. This is true, even if one compares similar data from one set of experiments in one laboratory. For example, the data set for different frequencies and fixed fluence in Fig. 1 shows the mixed influence of change in irradiation frequency and systematic changes of pulse shape with changes in laser frequency. The latter changes depend upon the characteristics of the pulses and thus upon the laser used and are, therefore, not transferable from one laboratory to another. On the other hand, the rate coefficients to be discussed next are transferable to a good approximation [4] [16].

3.3. *Determination of $k(st)$* . The steady-state rate coefficient was determined from the fluence dependence of the total product yield irradiation at 1087 cm^{-1} (9R34), using the

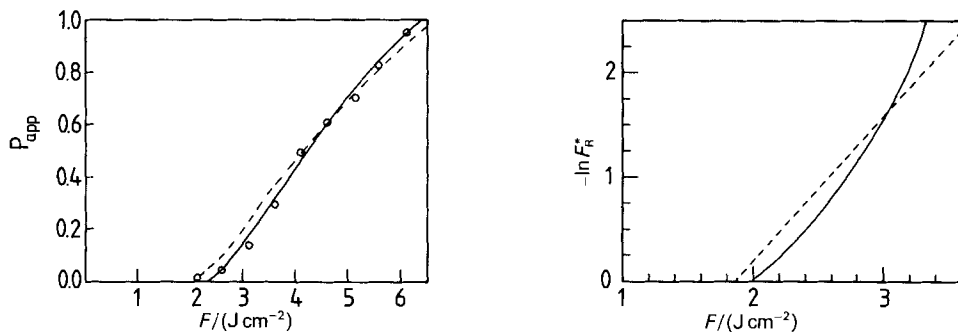


Fig. 3. a) Experimental data points (o) for P_{app} and best fits to the data for the irradiation of $\text{CHFCl}-\text{CF}_2\text{Cl}$ at 1087 cm^{-1} (9R34). b) The true yield function $-\ln F_R$ calculated from the best fits to the data. The full line — is for two exponentials, the dashed line - - - is for one exponential (see detailed discussion in the text).

data analysis routine described in [6]. A Gaussian shape function was used for the spatial fluence profile. Fluence was varied by positioning the sample cell varying distances from an $f = 5\text{ m}$ molybdenum mirror; the discharge voltage and total pulse energy were kept nearly constant to avoid systematic changes in the temporal pulse shape. Fig. 3 shows the experimental results and two fits to the measured P_{app} . Both curves fit P_{app} by expressions for the fraction of remaining reactant F_R of the form [6]

$$F_R^{(\nu)} = \sum_i \phi_i \exp(\kappa_i t) \quad (19)$$

with $-\kappa_1 = k(st)/I$. A sum of two exponentials (solid line) yielded the better fit to the data, with a value for the rate coefficient of $k(st) = 1.0 \cdot 10^6\text{ (I/MWcm}^{-2}\text{)s}^{-1}$. The two exponential fit gave, however, as well $\kappa_2 > 0$, which is a nonphysical result, as one requires in principle $\kappa_2 < \kappa_1 \leq 0$ [17]. The one exponential fit is not as good at low yields, as may be expected, but yields a similar rate coefficient $k(st) = 1.4 \cdot 10^6\text{ (I/MWcm}^{-2}\text{)s}^{-1}$. We also attempted to fit the data to a basis function arising from the activation equation [6] [18]

$$k(t) = k(st) \exp[-(\theta/t)^2] \quad (20)$$

but these fits were poor, did not converge well and yielded a clearly unreasonable value of $k(st) = 7.1 \cdot 10^7\text{ (I/MWcm}^{-2}\text{)s}^{-1}$. We consider the exponential fits to be more reliable, and report as a best value

$$k(st) = 10^{6.1 \pm 0.3}\text{ (I/MWcm}^{-2}\text{)s}^{-1} \quad (21)$$

The error limits of a factor of two include allowances for systematic errors and nonideality of the model functions for describing this system. We note that the root mean square deviations of the fits are well within the experimental error and the statistical error is smaller than a factor of two.

Although $k(st)$ is determined by bulk photolysis without time resolution at a pressure where the collisional frequency is high, the apparent $k(st)$ measured here corresponds to the collisionless $k(st)$ which would be observed with time resolution at low pressure [6]. Model calculations demonstrating this correspondence have been presented in [6]. Thus, we determine from bulk measurements the fundamental kinetic quantity of an absolute rate coefficient. The physical significance of $k(st)$ becomes clear, if we imagine a time-resolved experiment, in which $\text{CHFCl}-\text{CF}_2\text{Cl}$ is irradiated by IR laser light with a constant

intensity of 80 MWcm^{-2} , which corresponds to a typical average intensity for IR photochemistry. After the steady state is reached, one would observe primary decay of reactant into all primary chemical channels with a unimolecular total reactant rate constant of

$$k_{\text{uni}}(\text{st}) = 1.0 \cdot 10^8 \text{ s}^{-1} \quad (22)$$

3.4. Band Intensities for the C–F Chromophore and Comparison of $k(\text{st})$ with Theoretical Estimates. Theoretical calculations of unimolecular reactions induced by monochromatic infrared radiation (URIMIR) in the case B limit [16] [17] have shown the dependence of $k(\text{st})$ on reaction threshold and zero-point vibration energies E_{T} and E_{Z} , the number of vibrational degrees of freedom s , the excitation quantum $\tilde{\nu}_i$, and the integrated IR chromophore band strength G , defined as

$$G = \int_{\text{band}} \sigma(\tilde{\nu}) \frac{d\tilde{\nu}}{\tilde{\nu}} \quad (23)$$

with the *Lambert-Beer* absorption cross section from $\ln(I_0/I) = \sigma cl$, where concentration c is in particles per unit volume and l is the absorption path length. We have developed a simple analytical expression which depends explicitly on these molecular parameters and which accurately reproduces the values of $k(\text{st})$ obtained from the full statistical model calculations. This equation takes the following general form [4] [21]:

$$\frac{k(\text{st})/\text{s}^{-1}}{(I/\text{MWcm}^{-2})} = \frac{\alpha' s^a \tilde{\nu}_i^b G'}{\Delta\tilde{\nu}'[(E_{\text{T}}' + AE_{\text{Z}}')f(E_{\text{T}}', E_{\text{Z}})]} \quad (24)$$

where the primes indicate reduced units such as $G' = G/\text{pm}^2$, etc., and $\Delta\tilde{\nu}$ is the coupling width [17] [18]. A and $f(E_{\text{T}}, E_{\text{Z}})$ are corrections arising from different density of states expressions. In simple cases, A is equal to zero or one, but it can also be the *Whitten-Rabinovitch* correction factor [19] or a semiempirical adjustable parameter. The function $f(E_{\text{T}}, E_{\text{Z}})$ may be set equal to one or may take the form of the *Haarhoff* correction to the semiclassical density of states expression [20]:

$$f(E_{\text{T}}, E_{\text{Z}}) = \left[1 - A_1 \left(\frac{E_{\text{Z}}}{E_{\text{T}} + E_{\text{Z}}} \right)^2 + A_2 \left(\frac{E_{\text{Z}}}{E_{\text{T}} + E_{\text{Z}}} \right)^4 + \dots \right] \quad (25)$$

The coefficients A_1 , A_2 , etc. may be calculated from the *Haarhoff* expressions or the series may be truncated after two terms and A_1 treated as a parameter.

A crucial quantity in Eqn. 24 is the integrated chromophore band strength, which we have determined for $\text{CHFCl}-\text{CF}_2\text{Cl}$. Fig. 4 shows an FTIR spectrum of this molecule from 760 to 1400 cm^{-1} , recorded at a resolution of 0.05 cm^{-1} . The C–F chromophore dominates the molecular absorption between 900 and 1400 cm^{-1} . Table 1 shows the measured integrated band strengths from 941 to 1370 cm^{-1} . Although the total value of $G = 8.2 \text{ pm}^2$ is greater than three times 1.7 pm^2 , the predicted value from group additivity in the chromophore model [22], it is still of the expected order of magnitude. There exist to our knowledge no previous measurements of integrated band strengths for this molecule.

The correct choice of the effective G for IR multiphoton excitation at 1087 cm^{-1} is not obvious for $\text{CHFCl}-\text{CF}_2\text{Cl}$. One extreme (case *i*) is to consider only the band nearest the laser line from 1083 – 1123 cm^{-1} to be effectively coupled to the radiation field; this assumption gives an effective G of 1.5 pm^2 . This limit seems to be too extreme, as the three

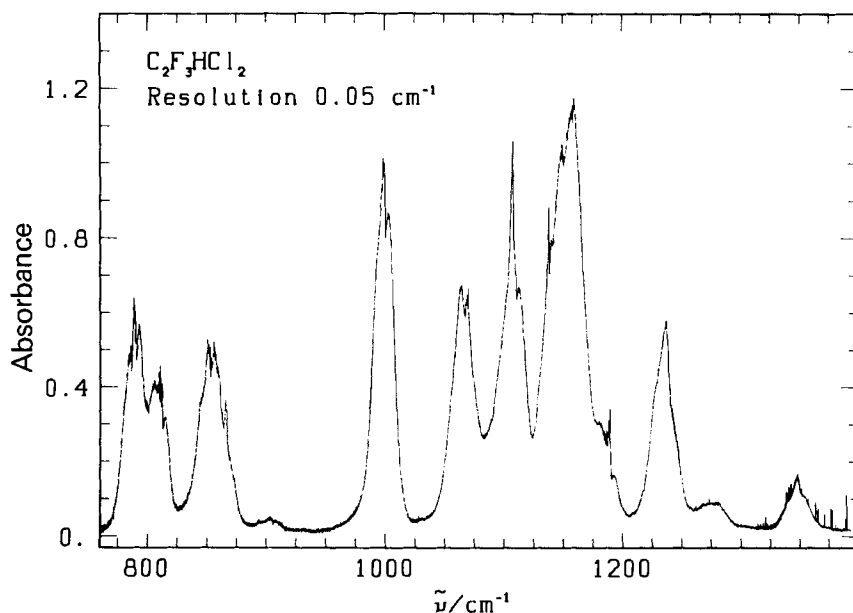


Fig. 4. FTIR spectrum of 3-mbar $\text{CHFCl}-\text{CF}_2\text{Cl}$ (17 cm) from 760 to 1400 cm^{-1} at a resolution of 0.05 cm^{-1}

Table 1. Measured Band Strengths of $\text{C}_2\text{F}_3\text{HCl}_2$ in the C-F Chromophore Region. Determined with and without Added N_2 , at a Resolution of 0.1 cm^{-1}

$\tilde{\nu}_{\text{band}}/\text{cm}^{-1}$	$\tilde{\nu}_{\text{max}}/\text{cm}^{-1}$	G/pm^2
941-1025	999	1.54 ± 0.03
1025-1083	1064	1.19 ± 0.03
1083-1123	1106	1.48 ± 0.04
1123-1205	1158	3.02 ± 0.04
1205-1310	1235	0.95 ± 0.06
		Total 8.2

bands between 1025 and 1205 cm^{-1} are poorly separated. An upper limit for G (case *ii*) is obtained by treating the entire chromophore region, with $G = 8.2 \text{ pm}^2$, as effectively coupled. A reasonable intermediate value (case *iii*) is obtained by summing the strengths of the bands from 1025 to 1205 cm^{-1} which gives $G = 5.6 \text{ pm}^2$.

We show in Table 2 a comparison of the experimental $k(\text{st})$ and theoretical estimates based on the assumptions about G discussed above and using three variations of Eqn. 24 and parameters α , a, b, c and when applicable A and A_1 optimised to a data set of exact results for molecules with 8 atoms or fewer [21]. The theoretical values agree quite well with the experimental $k(\text{st})$, particularly for the reasonable case *iii* assumption of $G = 5.6 \text{ pm}^2$. The uncertainty in the choice of effective G creates, however, a significant uncertainty in the theoretical estimates, which is larger than the uncertainties arising because of the simple theoretical equations, experimental data, or estimates for the threshold and zero-point energies. Thus the agreement between experiment and theoretical estimate should not be overemphasized.

Table 2a. *Parameters Used for Theoretical Estimates of k(st). Eqn. a, b, and c are three different versions of Eqn. 24, with parameters as given above. Eqn. c is with f(E_T, E_Z) truncated after the A₁ term. The value for E_T was estimated [11]. E_Z was taken as the value for CCl₂H–CF₃, as the only report of an IR spectrum of CHFCI–CF₂Cl [8] contains no vibrational analysis.*

	Eqn. a	Eqn. b	Eqn. c
E _T /1000 cm ⁻¹	20.9	20.9	20.9
E _Z /1000 cm ⁻¹	7.49	7.49	7.49
$\bar{\nu}_1$ /1000 cm ⁻¹	1.09	1.09	1.09
s	18	18	18
α'	4.46 · 10 ⁶	6.74 · 10 ⁶	6.54 · 10 ⁶
a	1.90	1.16	1.47
b	2.20	2.12	2.16
c	2.61	2.02	2.27
A	1	0.47	1
A ₁	0	0	0.57

Table 2b. *Comparison of the Experimental Rate Coefficient with Theoretical Estimates (with an empirical value of $A\bar{\nu} \approx 0.25 \bar{\nu}$, see [2]). The values of G were chosen according to the assumptions i, ii, and iii described in the text.*

	$k(st)/s^{-1}$ I/MW cm ⁻¹
Experiment	1.2 · 10 ⁶
Case i, Eqn. a	0.41 · 10 ⁶
Case ii, Eqn. a	2.24 · 10 ⁶
Case iii, Eqn. a	1.53 · 10 ⁶
Case iii, Eqn. b	1.21 · 10 ⁶
Case iii, Eqn. c	1.28 · 10 ⁶

We thank R. O. Kühne and Georg Seyfang for assistance and for helpful discussion. Our work is supported financially by the Schweizerischer Nationalfonds zur Förderung der wissenschaftlichen Forschung and the Schweizerischer Schulrat.

REFERENCES

[1] P. A. Schulz, Aa. S. Sudbo, D. J. Krajnovich, H. S. Kwok, Y. R. Shen, Y. T. Lee, *Ann. Rev. Phys. Chem.* **1979**, 30, 379.
 [2] M. Quack, *Chimia* **1981**, 35, 463.
 [3] M. Quack, *Adv. Chem. Phys.* **1982**, 50, 395.
 [4] D. Lupo, M. Quack, *Chem. Rev.* **1987**, in press.
 [5] M. Quack, *J. Chem. Phys.* **1979**, 70, 1069.
 [6] M. Quack, G. Seyfang, *J. Chem. Phys.* **1982**, 76, 955.
 [7] M. Quack, E. Sutcliffe, P. Hackett, D. Rayner, *Faraday Disc. Chem. Soc.* **1986**, in press.
 [8] P. Hackett, D. Rayner, M. Quack, E. Sutcliffe, to be published.
 [9] a) J. D. Park, W. R. Lycan, J. R. Lacher, *J. Am. Chem. Soc.* **1951**, 73, 711; b) M. C. Bindal, P. Singh, H. Gupta, *Drug Res.* **1980**, 30, 234; c) P. Ruelle, C. Sandorfy, *Int. J. Quantum Chem.* **1982**, 21, 691.
 [10] T. Yano, E. Tschuikow, *J. Chem. Phys.* **1980**, 72, 3401.
 [11] S. W. Benson, 'Thermochemical Kinetics', John Wiley and Sons, New York, 1976, 2nd edn.
 [12] R. J. S. Morrison, R. F. Farley, E. R. Grant, *J. Chem. Phys.* **1981**, 75, 148.
 [13] J. W. Hudgens, *J. Chem. Phys.* **1978**, 68, 777.
 [14] D. Krajnovich, F. Huisken, Z. Zhang, Y. R. Shen, Y. T. Lee, *J. Chem. Phys.* **1982**, 77, 5977.
 [15] M. Quack, G. Seyfang, *Ber. Bunsenges. Phys. Chem.* **1982**, 86, 504.
 [16] P. Gozel, H. van den Bergh, D. Lupo, M. Quack, G. Seyfang, to be published.
 [17] M. Quack *J. Chem. Phys.* **1978**, 69, 1282; M. Quack, *Ber. Bunsenges. Phys. Chem.* **1979**, 83, 757.
 [18] M. Quack, *Ber. Bunsenges. Phys. Chem.* **1979**, 83, 1287.
 [19] E. Z. Whitten, B. S. Rabinovitch, *J. Chem. Phys.* **1963**, 38, 2466.
 [20] P. C. Haarhoff, *Mol. Phys.* **1963**, 6, 337; *ibid.* **1963**, 7, 101.
 [21] D. W. Lupo, M. Quack, to be published.
 [22] M. Quack, H. J. Thöne, *Ber. Bunsenges. Phys. Chem.* **1983**, 87, 582.